JOURNAL OF APPLIED ELECTROCHEMISTRY 26 (1996) 1195–1199

Electrocatalytic properties of ternary oxide mixtures of composition $Ru_{0.3}Ti_{(0.7-x)}Ce_xO_2$: oxygen evolution from acidic solution

L. A. DE FARIA

Instituto de Química de São Carlos, Universidade de São Paulo, Caixa Postal 369, 13560-970 São Carlos, S.P., Brazil

J. F. C. BOODTS

FFCLRP, Departamento de Química, Universidade de São Paulo, Av. Bandeirantes 3900, 14040-901 Ribeirão Preto, S.P., Brazil

S. TRASATTI

Department of Physical Chemistry and Electrochemistry, University of Milan, Via Venezian 21, 20311 Milan, Italy

Received 3 January 1995; revised 9 October 1995

Mixed oxide electrodes of general composition $Ru_{0.3}Ti_{(0.7-x)}Ce_xO_2$ were prepared by thermal decomposition of the respective chlorides using Ti as a support. x was varied between 0 and 70 mol %. Oxygen evolution was used as a model reaction to investigate the dependence of the electrocatalytic properties on oxide composition. Kinetics was studied by quasistationary current–potential curves and reaction order determination. A minimum Tafel slope of about 30 mV has been found in the 10–30% CeO_2 composition range. On the basis of a zero reaction order at constant overpotential, a reaction mechanism has been proposed accounting for the composition dependence of the Tafel slope. It has been concluded that the replacement of TiO_2 with CeO_2 brings about an increase in the electrocatalytic activity for oxygen evolution, while the layer becomes more prone to mechanical erosion.

1. Introduction

Industrial anodes have been traditionally based on $RuO_2 + TiO_2$ mixtures whose activity is provided by RuO_2 while TiO_2 imparts its chemical inertness to the system. For more specific applications, additives are necessary either to improve the selectivity or to enhance the stability.

CeO_2 is in principle an interesting candidate as an additive. Its high Ce(III)/Ce(IV) redox potential is expected to depress the reactivity for oxygen evolution of anodes for the chlor–alkali cells [1], while for the same reason it is expected to impart chemical inertness to an oxide mixture. Although mentioned in a few patents [1, 2], fundamental research on CeO_2-containing electrodes is scanty in the literature [3]. Recently, we have studied the physicochemical and electrochemical surface properties of the system $RuO_2 + TiO_2 + CeO_2$ [4]. In this paper, for the same system we shall discuss electrocatalytic and mechanistic aspects of the oxygen evolution reaction from acidic solution.

2. Experimental details

2.1. *Electrodes*

Mixed oxide layers were deposited on 10 mm × 0.15 mm Ti supports by thermal decomposition at 450 °C of mixtures of $RuCl_3 \cdot nH_2O$ (Aldrich), $TiCl_4$ (Ventron) and $CeCl_3 \cdot 7H_2O$ (Merck) in an oxygen atmosphere (5 dm^3 min^{-1}). The details of the procedure have been described previously [4]. The oxide loading was 2 to 2.8 mg depending on composition (corresponding to a nominal thickness of 2 μm).

Samples of nominal composition $Ru_{0.3}Ti_{(0.7-x)}Ce_xO_2$ were prepared at 10 mol % intervals (except for 5% CeO_2), two samples at each composition. The electrodes were mounted in Teflon holders as illustrated elsewhere [5]. Solutions were prepared volumetrically using $HClO_4$ (Merck) and triple distilled water; they were deaerated before and during each experiment using purified nitrogen gas. The temperature was maintained at 25° C by means of a water thermostat. The three-compartment cell has been described in a previous paper [6].

Electrode potentials were read against a hydrogen electrode in the same solution and are reported on the (RHE) scale.

2.2. *Methods*

PAR instrumentation was used throughout. Electrodes were studied by cyclic voltammetry and steady-state potentiostatic curves. Voltammetric

0021-891X

curves were recorded at $20\,mV\,s^{-1}$ in the potential range 0.9–1.4 V vs RHE. The voltammetric charge spent in this potential range was determined by integration of the j/E curves using a digitizing device.

Potentiostatic curves were recorded keeping the electrode at 1.2 V for 15 min; then moving the potential anodically, first in 50 mV steps until 1.35 V and then in 10 mV steps until the current reached a value of approximately 100 mA. The current was read after 3 min at each potential.

Reaction order experiments were performed by keeping the electrode at 1.25 V for 15 min, then stepping the potential to 1.51 V for an additional 15 min, and finally stepping to the selected potential of 1.43 V vs RHE, where the current was recorded as a function of time. Experiments were carried out with solutions at several different pH values obtained by changing the composition of the electrolyte, x mol dm^{-3} $HClO_4 + (1-x)$ mol dm^{-3} $NaClO_4$, between $x = 0.1$ and $x = 1$ at constant ionic strength (1 mol dm^{-3} ClO_4^-). The potential of 1.43 V vs RHE was chosen because it was observed to fall on the linear portion (Tafel line) of the experimental curve for all electrodes.

3. Results

3.1. *Tafel lines*

For each electrode current–potential curves were recorded twice (forward and backward) without interruption. With freshly prepared electrodes the first run ('up' and 'down'), produced curves exhibiting a small amount of hysteresis. In the second run, the hysteresis was negligible. Polarization curves, after ohmic drop correction, generally showed more than one Tafel line, with the possible exception of the electrode without TiO_2. A typical curve (second run) is shown in Fig. 1.

Figure 2 shows the dependence of the Tafel slopes on oxide composition. At low overpotentials the Tafel slope falls in the range from 30 to 40 mV. There is a minimum at 30 mV for CeO_2 contents ranging

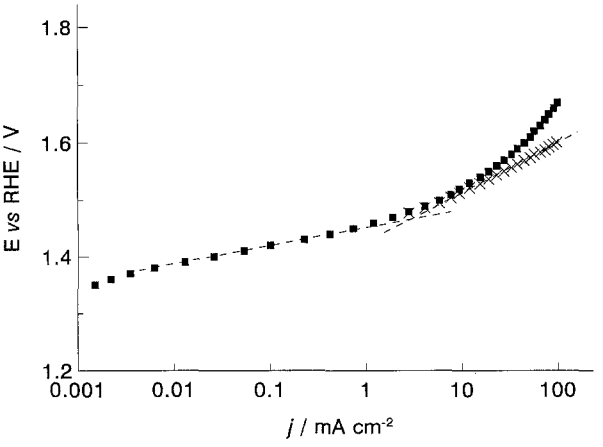

Fig. 1. Current–potential curve for oxygen evolution on $Ru_{0.3}Ti_{0.4}Ce_{0.3}O_2$ electrode from 1 mol dm^{-3} $HClO_4$ solution, second run. (×) Data corrected for ohmic drop.

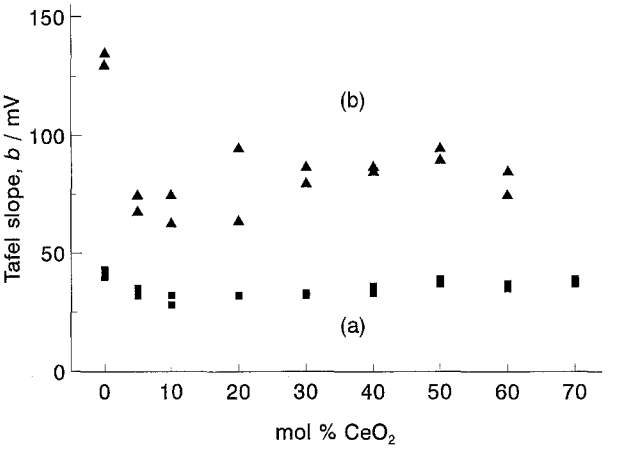

Fig. 2. Tafel slope as a function of oxide composition for oxygen evolution from 1 mol dm^{-3} $HClO_4$ solution. (a) Low overpotentials; (b) high overpotentials.

10–30 mol %. The slope of 40 mV for the binary $RuO_2 + TiO_2$ electrode was also observed by other workers, but the introduction of a small amount of CeO_2 reduces the Tafel slope appreciably. The Tafel slope increases at higher CeO_2 contents than 30 mol % again reaching 40 mV for the RuO_2+ CeO_2 binary system.

At higher overpotentials, a second Tafel line appears whose slope changes from about 120 mV for the binary electrode without CeO_2 down to about 70 mV with only 5% CeO_2. Despite a small oscillation paralleling that visible at lower current densities, the second Tafel slope does not vary appreciably with further increase in CeO_2 content, being between 60 and 85 mV.

3.2. *Reaction order*

Figure 3 shows the dependence of the rate of oxygen evolution on the solution pH at constant ionic strength. Within experimental error, the current does not vary with pH.

Therefore, $\partial \log j/\partial \mathrm{pH} = 0$. Since the reference electrode was a hydrogen electrode in the same solution, the observed reaction order is, in fact, at *constant*

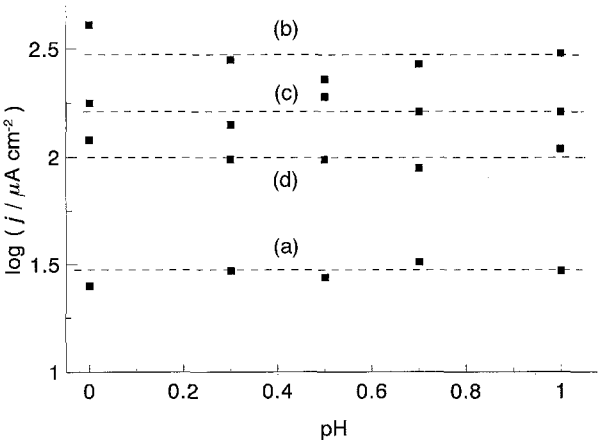

Fig. 3. Dependence of current density at 1.43 V vs RHE on pH for oxygen evolution on $Ru_{0.3}Ti_{(0.7-x)}Ce_xO_2$ electrodes from 1 mol dm^{-3} ($HClO_4 + NaClO_4$ solutions). (a) $x = 0$; (b) $x = 0.1$; (c) $x = 0.5$ and 0.6; (d) $x = 0.7$ mol %.

overpotential and not at constant potential. Only the reaction order at *constant potential* is chemically significant.

The relation between the two reaction orders is as follows:

$$_{\eta}\nu = {}_{E}\nu - \gamma \tag{1}$$

where η is the overpotential, ν the reaction order and γ the factor in the denominator of the Tafel slope ($RT/\gamma F$). Therefore,

$$_{E}\nu(\mathrm{pH}) = {}_{\eta}\nu(\mathrm{pH}) + \gamma \tag{2}$$

Since, for all electrodes, $_{\eta}\nu = 0$, then

$$_{E}\nu(\mathrm{pH}) = \gamma \tag{3}$$

With a Tafel slope of 40 mV, $\gamma = 1.5$, while with a Tafel slope of 30 mV, $\gamma = 2$. Therefore, the reaction order at constant potential varies with the oxide composition in parallel with the Tafel slope between -1.5 and -2.

3.3. *Electrocatalytic activity*

Since the voltammetric charge (i.e., the active surface area) is a function of the oxide composition, true electrocatalytic effects can be disentangled only by normalizing the current to unit active surface area. Figure 4 shows a plot of the (true) activity (current density) at 1.43 V vs RHE against oxide composition.

The (j/q^*) plot at constant potential shows a sort of 'volcano' shape typical of electrocatalytic phenomena, which can be understood in terms of the S–OH bond strength depending on the CeO_2 content [7].

Maximum activity is observed at 10 mol % CeO_2. At lower contents, the S–OH bond strength is probably too weak, whereas at higher CeO_2 contents it is possibly too strong. It is interesting that the maximum in activity for oxygen evolution is observed at the same composition at which a minimum in activity is observed for chlorine gas evolution [8].

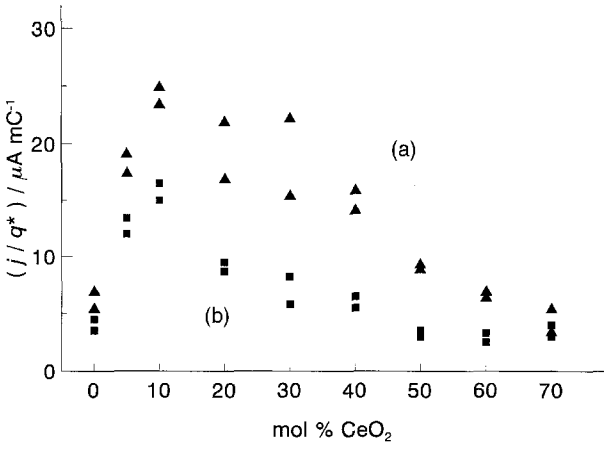

Fig. 4. Dependence of normalized current on oxide composition for oxygen evolution from 1 mol dm^{-3} $HClO_4$ solution. (a) Data from order of reaction, different sets of electrodes; (b) data from Tafel lines, different sets of electrodes.

3.4. *Uncompensated ohmic drop*

Experimental log j/E curves were corrected for uncompensated ohmic drops using two graphical indirect methods. In one case, ΔE data were calculated at each value of current from the difference between the experimental point and the extrapolated Tafel line based on the linearity of the data points at low currents. $\Delta E/I$ plots were then constructed and analysed according to the method proposed by Shub *et al.* [9].

In the second case, assuming a linear Tafel line, it is possible to write

$$E = a + b \ln I + RI \tag{4}$$

Differentiating with respect to current,

$$\frac{\partial E}{\partial I} = \frac{b}{I} + R \tag{5}$$

Thus, a plot of $\Delta E/\Delta I$ against $1/I$ should give straight lines of slope b and intercept R (for $I \to \infty$). Figure 5 shows that both approaches give the same results which can thus be considered as reliable.

The ohmic component in the oxide layer is seen to remain constant up to about 40 mol % CeO_2, then it increases by a factor of approximately two. At the lower CeO_2 content, the structure and the electrical properties of the oxide layer are dominated by the TiO_2 component which is doped by RuO_2. As the TiO_2 component becomes less than about 30%, the properties of CeO_2 become predominant. CeO_2 does not crystallize with the same crystal habit as RuO_2. CeO_2 is cubic whereas RuO_2 is tetragonal (rutile). Therefore, CeO_2 is not expected to form solid solutions with RuO_2, which explains why the ohmic resistance of the oxide layer increases at the higher CeO_2 contents.

3.5. *Electrode stability*

The determination of the voltammetric charge before

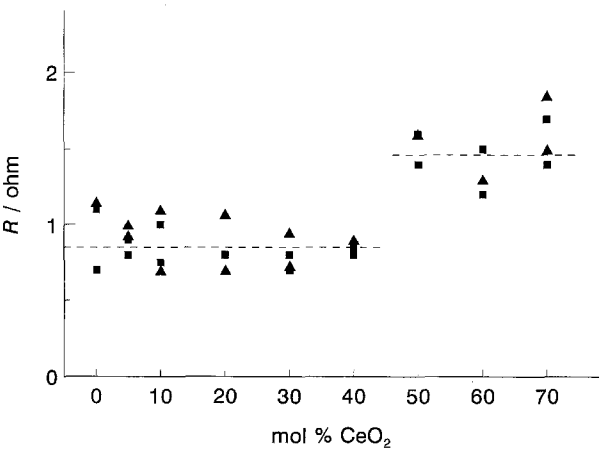

Fig. 5. Dependence of ohmic drop on oxide composition. (Δ) Data from Tafel lines calculated according to the method proposed by Shubs *et al.* [9].

and after each series of experiments allows an analysis of the electrode stability [10]. In this work, the voltammetric charge was measured with fresh electrodes, and again before and after each group of experiments (namely, Tafel line and reaction order determinations).

Figure 6 shows the voltammetric charge as a function of oxide composition. It is interesting that the charge is not appreciably different after the Tafel slope determination, while a detectable decrease in q^* (i.e., a decrease in the active surface area) is observed after the reaction order experiments.

This is possibly due to the sudden change in potential with consequent gas evolution which can disrupt the pore structure. Conversely, since Tafel lines are recorded with a progressive increase in potential, gas evolution inside the pores does not take place abruptly with consequent mechanical stress. At any rate, no instability is observed with $RuO_2 + TiO_2$ electrodes.

4. Discussion

Oxygen evolution on $RuO_2 + TiO_2 + CeO_2$ ternary oxides takes place with a mechanism which depends on the oxide composition and the potential range. Experimental polarization curves generally show more than one Tafel line, with the possible exception of the electrode without TiO_2.

The slope of 40 mV suggests a mechanism where the second electron transfer is rate determining. The slope of 30 mV is characteristic of a recombination reaction. Thus, a general mechanism may be the following (S is a surface active site):

(a) $S + H_2O \longrightarrow S\text{–}OH + H^+ + e^-$
(b) $S\text{–}OH \longrightarrow S\text{–}O + H^+ + e^-$
(b′) $S\text{–}OH + S\text{–}OH \longrightarrow S\text{–}O + H_2O$
(c) $S\text{–}O + S\text{–}O \longrightarrow 2S + O_2$

In the above mechanism steps (b) and (b′) are alternative, i.e. they occur in parallel, the occurrence of one or the other depending on the adsorption strength of the intermediate.

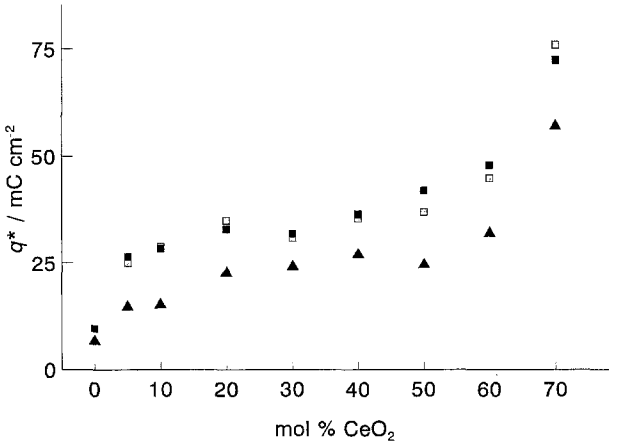

Fig. 6. Voltammetric charge (q^*) as a function of oxide composition from 1 mol dm^{-3} $HClO_4$ solution. (■) Fresh electrodes; (□) after extensive oxygen evolution; (▲) after the final reaction order experiment.

The analysis developed by Parsons [11] for the hydrogen evolution reaction on metals can be extended to this case if H is replaced by OH as the intermediate. Thus, it can be argued that the mechanism changes with oxide composition as a consequence of a variation in the S–OH bond strength. In the absence of CeO_2 step (b), as usually observed, is rate determining. The introduction of CeO_2 appears to strengthen the S–OH surface bond. This leads to an increase in the intermediate surface coverage as a result of which the preferred pathway is now via step (b′). Since further addition of CeO_2 increases the bond strength further, step (b′) will be slowed down becoming step (b) again rate determining.

At higher overpotentials, the second Tafel slope, obtained after ohmic drop correction, is more difficult to interpret since its value is not a 'standard' one. It is possible that the intermediate OH is first formed as an unstable species which rearranges via a surface reaction (spillover). Thus, step (a) in the general mechanism may be substituted by the following steps:

(a) $S + H_2O \longrightarrow S\text{–}OH^* + H^+ + e^-$
(a′) $S\text{–}OH^* \longrightarrow S\text{–}OH$

where the asterisk marks a different energy state. At high overpotentials, step (a′) may become slow and the Tafel slope becomes about 60 mV. Alternatively, step (a) may become the slowest and the Tafel slope becomes 120 mV. Intermediate values of Tafel slope may be interpreted in terms of mixed kinetic control [12].

Although the predicted and the observed reaction orders coincide ($\nu = -2$) as the Tafel slope is 30 mV, the reaction order of -1.5 differs from the predicted value of -1. Fractional reaction orders have often been observed for oxygen evolution on oxide electrodes and have been interpreted in terms of acid–base equilibria at the oxide surface [13, 14]. Under similar circumstances the electrical potential at the surface sites becomes a function of pH: the higher the acidity (the lower the pH) the more positive (or the less negative) the potential at the oxide surface.

If step (b) in the mechanism shown above is rate determining, as demonstrated in a previous paper, the reaction order with respect to H^+ turns out to be $-(1 + \alpha)$; that is, -1.5 with $\alpha = 0.5$.

The observed reaction orders are, therefore, consistent with the reaction orders predicted by the mechanism proposed above. Also, the activity data are perfectly consistent with the discussion of the mechanism.

5. Conclusions

The presence of CeO_2 with TiO_2 increases the electrocatalytic activity of RuO_2-based electrodes for oxygen evolution. At the same time, CeO_2 gives rise to a more fragile structure of the oxide layer which is thus more prone to mechanical erosion generated by gas evolution reactions.

Acknowledgements

J. F. C. Boodts wishes to acknowledge the financial support received from the FAPESP Foundation and the PADCT II/CNPq. S. Trasatti is grateful to C.N.R. (Rome) for financial support.

References

[1] S. Saito, M. Kobayashi and Y. Kawai, *Japan, Kokai Tokyo Koho* **78** (1978) 33983; *Chem. Abstr.* **89** (1978) 97165.
[2] A. Nakamura and S. Saito, *ibid.* **79** (1978) 202209; *Chem. Abstr.* **91** (1979) 219421.
[3] L. Kühnemund, H. Heidrich, R. Sabela, L. Stephan and L. Müller, *Z. Phys. Chem.* **271** (1990) 901.
[4] L. A. de Faria, J. F. C. Boodts and S. Trasatti, *Electrochim. Acta* **37** (1992) 2511.
[5] R. Garavaglia, C. M. Mari and S. Trasatti, *Surf. Technol.* **23** (1984) 41.
[6] G. Lodi, E. Sivieri, A. De Battisti and S. Trasatti, *J. Appl. Electrochem.* **8** (1978) 135.
[7] S. Trasatti, *J. Electroanal. Chem.* **111** (1980) 125.
[8] L. A. de Faria, J. F. C. Boodts and S. Trasatti, to be submitted.
[9] D.M. Shub, M.F. Reznik and V. V. Shalaginov, *Electrokhimiya* **221** (1985) 937.
[10] S. Trasatti, *Elektrochim. Acta* **36** (1991) 225.
[11] R. Parsons, *Trans. Faraday Soc.* **54** (1958) 1053.
[12] J. O'M. Bockris, *J. Chem. Phys.* **24** (1956) 817.
[13] C. Angelinetta, M. Falciola and S. Trasatti, *J. Electroanal. Chem.* **205** (1986) 347.
[14] L .I. Krishtalik, *Electrochim. Acta* **26** (1981) 329.